Application of microbially induced carbonate precipitation (MICP) to form bio-cemented artificial sandstone

Charalampos Konstantinou[1], Giovanna Biscontin[2], Ning-jun Jiang[3], and Kenichi Soga[4]

[1]Department of Engineering, University of Cambridge, UK (corresponding author). Email: ck494@cam.ac.uk Tel:+447746388051 ORCID: https://orcid.org/0000-0002-4662-5327

[2]Department of Engineering, University of Cambridge, UK. Email: gb479@cam.ac.uk ORCID: https://orcid.org/0000-0002-4662-5650

[3]Department of Civil and Environmental Engineering, University of Hawaii at Manoa, Honolulu, HI 96822, USA. Email: jiangn@hawaii.edu ORCID: https://orcid.org/0000-0001-6070-4307

[4]Department of Civil and Environmental Engineering, University of California, Berkeley, CA 94720, USA. Email: soga@berkeley.edu

ABSTRACT

It is difficult to collect and characterise well-preserved samples of weakly cemented granular rocks as conventional sampling techniques often result in destruction of the cementation. An alternative approach is to prepare synthetic geomaterials to match required specifications. This paper introduces microbially induced carbonate precipitation (MICP) as a method to reliably deliver artificially cemented specimens with customised properties, closely resembling those of soft carbonate sandstones. The specimens are generated from materials with two very different particle size distributions to access a range of achievable combinations of strengths and porosities. The MICP parameters are kept constant across all samples to obtain similar calcium carbonate characteristics (size of individual crystals, type etc.), while injected volume is varied to achieve different cementation levels. Although uniform cementation of very coarse sands has been considered very difficult to achieve, the results show that both the fine and coarse sand specimens present high degrees of uniformity and a good degree of repeatability. The strengths (UCS values less than 3000 kPa) and porosities (0.25-0.4) of the artificial specimens fall in the same range of values reported for natural rocks. The strength

gain was greater in the fine sand than in the coarse sand, as the void size in the latter was significantly larger compared to the calcium carbonate crystals' size, resulting in precipitation on less effective locations, away from contacts between particles. The strengths and porosities obtained for the two sands in this work fall within ranges reported in the literature for natural soft rocks, demonstrating the MICP technique is able to achieve realistic properties and may be used to produce a full range of properties by varying the grain sizes, and possibly the width of the particle size distribution.

KEYWORDS

Granular rocks, biocementation, MICP, grain size, uniformity, efficiency, artificial rock

LIST OF SYMBOLS

UCS	Unconfined compressive strength
MICP	Microbially induced carbonate precipitation
OD	Optical density
CS	Cementation solution
BS	Bacteria solution
D_{50}	Mean particle size
LNB	Liquid nutrient broth
n	Porosity
I_s	Point load index
PSD	Particle size distribution

1. INTRODUCTION

The term soft sandstone is used in reference to poorly consolidated weakly cemented sandstones, representing a transitional material between soils and fully aggregated rocks, and

sharing characteristics and behavior of both (Sitar et al. 1980; Collins and Sitar 2009, Nakagawa and Myer 2001). Sandstones represent the host rock for a large portion of active aquifers and oil and gas reservoirs because their high porosity both enhances storage and facilitates extraction. The transitional nature of sandstones, in particular, presents some challenges to the safety of extraction operations and the mechanical response of these materials under a variety of conditions is still poorly understood. Unfortunately, coring of soft sandstones tends to destroy cementation resulting in poor recoveries, so that sufficient quantities of high-quality samples for laboratory testing are both difficult to obtain and expensive. As an alternative, synthetic rock specimens can provide virtually limitless quantities and customisable characteristics, allowing relevant structural parameters to be varied independently, and hence isolating their effects (Saidi et al. 2005). Rock specimen reproduction has received great attention in the literature (Wygal 1963; Maccarini 1987; Nakagawa and Myer 2001; Ismail et al. 2002; Saidi et al. 2003; Vogler et al. 2017) due to the increasing need for understanding the mechanical behavior of various rocks.

Soft sandstones are characterized by low unconfined compressive strength, poor core integrity, core wash-out during laboratory tests, and stress-dependent porosity and permeability. Studies report unconfined compression strength (UCS) values ranging from 100-3500 kPa (Sitar et al. 1980; Shafii Rad and Clough 1982; Dobereiner 1984; Ispas et al. 2012; Kanji 2014; Pradhan et al. 2014; Sattler and Paraskevopoulou 2019). Another critical property dominating the behaviour of these materials is porosity, generally ranging from 0.2 to 0.4, much higher than in competent rocks (Heath 1965; Sitar et al. 1980; Krishnan et al. 1998; Suarez-Rivera et al. 2002; Collins and Sitar 2009). As the value of porosity is determined by simple tests, it is often used to derive strength or permeability of the material from empirical relationships (Fjar et al. 2008). Any method that aims at reproducing salient properties of soft sandstones needs to reproduce the correct combination of strength and porosity.

Collins and Sitar (2009) demonstrated that the behaviour of most cemented sandstones appears to be similar regardless of the particular cementing agent, but the degree of cementation is closely linked to the mechanical properties. This study focuses on carbonate cemented sandstones.

Microbially induced carbonate precipitation (MICP) can be applied to produce a range of weak carbonate sandstone-like materials from a base sand through a bio-process that builds up calcium carbonate cementation around the particles. MICP is potentially an excellent tool to develop artificially carbonate cemented sandstone with consistent characteristics that can be customized by changing the amount of carbonate cementing agent. The main objectives of this study were: (1) to assess reliability and repeatability of the MICP process used to generate synthetic specimens with varying controllable properties from materials with different particle size distributions and (2) to determine whether the resulting properties, primarily strength and porosity, would sufficiently resemble weakly carbonate cemented sandstones to be used as a substitute in a subsequent laboratory investigation of mechanical response under more complex loading conditions.

2. BACKGROUND

MICP has been extensively studied for a number of geotechnical applications generally aimed at improving soil properties and reducing hazards such as: liquefaction control (Montoya et al. 2013; Montoya and DeJong, 2015), mitigation of internal and surface erosion (Jiang et al. 2017; Cheng et al. 2014; van Paassen et al. 2010), slope stabilisation (DeJong et al. 2010; DeJong et al. 2013), structural stability (Umar et al. 2016; Bella et al. 2017; Konstantinou and Biscontin 2020; DeJong et al. 2011), bio-remediation (Torres-Aravena et al. 2018; Li et al., 2013; Mugwar and Harbottle 2016) and even in self-healing of soils, bioconcrete or cracks (Harbottle et al. 2014; Montoya and Dejong 2013; Castro-Alonso et al. 2019; Ersan et al. 2016).

The advantage of the method over the conventional techniques is the mitigation of geotechnical

engineering problems in a non-disruptive manner. It can be easily applied at ambient temperatures over a large area, even under buildings, without disturbing them. MICP offers a substantial increase in strength, stiffness, and dilative behaviour, while retaining soil's permeability to some extent.

In MICP, bacteria are first introduced to the medium and then a cementation solution consisting of urea and a calcium source is supplied in the form of injections (Whiffin 2004; DeJong et al. 2006). The properties of the treated products, in particular strength and stiffness, depend on both the grain characteristics of the base material (particle roughness, shape, size) and the cement distribution and morphology within the medium (amount, crystal shape and size, and location of calcium carbonate) (DeJong et al. 2010; Mortensen et al. 2011; Al Qabany et al. 2012; Al Qabany and Soga 2013; Zhao et al. 2014; Cheng et al. 2017; Mujah et al. 2017). Although numerous studies have been conducted to derive protocols for effective bio-cementation by altering components of the MICP recipe (Whiffin et al. 2007; Al Qabany et al. 2012; Martinez et al. 2013; Cheng and Cord-Ruwisch 2014; Dawoud et al. 2014; Dawoud 2015; Feng and Montoya 2015; Cui et al. 2017; Jiang et al. 2017; Mujah et al. 2017; Cheng et al. 2019), cementation in the specimens has not always been uniform. This is an important consideration when using the method for artificial specimens' preparation as non-uniform samples invalidate any further testing results.

The focus of the majority of previous studies was the identification of the optimum protocol parameters. The granular material used was typically a single type of poorly graded fine sand with mean particle diameters of 0.15-0.7 mm (Zhao et al. 2014; Dawoud 2015; Feng and Montoya 2015; Lin et al. 2015; Cheng et al. 2017; Cui et al. 2017; Dadda et al. 2017, 2019). Coarse sand was very rarely selected for bio-cementation (Mahawish et al. 2018) due to size incompatibility between the microbes and the grain sizes according to the criterion proposed

by Mitchell and Santamarina (2005) (Fig. 1).

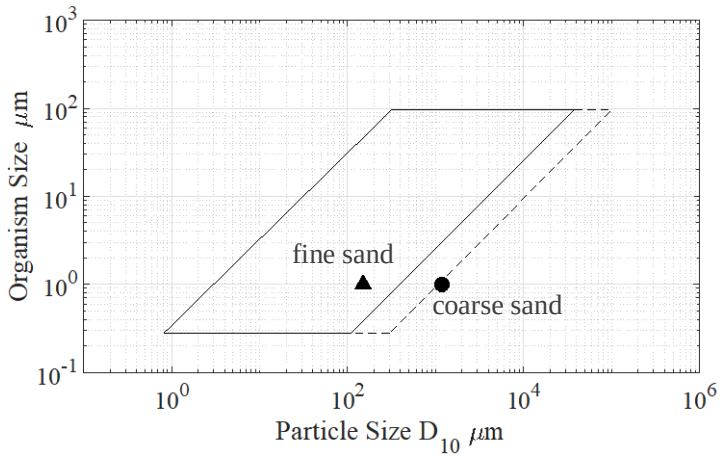

Fig. 1. The bounded region indicates the range of soil sizes that can be treated with bioclogging (after Mitchell and Santamarina, 2005)

Although it is generally recognised that the medium's intrinsic properties (grain size, roughness, particle's shape) affect the effectiveness of the process, the understanding of these effects remains limited. Rebata-Landa (2007) investigated the efficiency of MICP using different soils with varying grain sizes and porosity. In very fine soils, the bacterial activity (ability to metabolise and generate biofilms) was restricted by the small space available in the pores resulting in low calcium carbonate concentration. In coarse soils, the low cementation was attributed to the formation of a thin distributed layer of calcium carbonate, which was not sufficient to increase the strength of the specimens (Rebata-Landa 2007).

3. MATERIALS AND METHODS

The MICP procedure (bacterial density, urease activity, chemical concentration, injection times etc.) was identical for all specimens and all types of sand in order to minimise variability from bio-chemical processes, while the amount of cementation was varied by changing the amount of cementation solution injected into the medium. The key to obtaining uniform specimens of repeatable quality is to ensure that the bacteria and cementation solution are permeating the base material uniformly and the reactions occur at a rate that is compatible with the velocity of

the flow. Therefore, the effectiveness of the MICP process is controlled by chemical efficiency, which in turn depends on the retention times, the injecting method, the chemical concentration, and the optical density of the bacteria solution.

3.1. MICP Procedure

The bacterium *Sporosarcina pasteurii* was used, as its urease-synthesis behaviour is well-defined, and its activity has been proven to be higher than other species (Whiffin 2004). Batch experiments were conducted under aerobic conditions and in a sterile environment. The growing medium consisted of 20 g/L yeast extract, 10 g/L ammonium sulphate, 20 g/L agar, and 0.13 M tris buffer (base). After 24 h of incubation at 30 ˚C, the culture was harvested and stored at 4 ˚C. Bacterial colonies were introduced into liquid nutrient broth without agar (LNB), placed in a shaking incubator for additional 24 h to form the bacterial solution (BS), which was then stored at 4 ˚C. The optical density of the BS measured at a wavelength of 600 nm, OD_{600}, was between 1.5 and 2.0.

The bacterial urease activity for each specimen was measured with a conductivity assay (Whiffin, 2004) on a bacteria solution diluted to an optical density of 1.0 for the purpose of comparison with other works. The measured urease activity averaged across all tests, 0.8 (mM urea/h)/OD, was lower compared to most previous research (Whiffin et al. 2007; Cheng et al. 2013, 2017). However, it was sufficient to induce reactions in previous works (Jiang and Soga 2017) and was found to be a key factor in obtaining uniform specimens (Konstantinou, 2020).

The cementation solution (CS) used in this study comprised 0.375 M urea, 0.25 M calcium chloride ($CaCl_2$), and 3 g/L nutrient broth. This recipe was in the low range of concentrations among those reported in literature and applied longer retention times than most previous works, although it was consistent with several studies showing effective MICP treatment (DeJong et al. 2006).

3.2. Sample preparation

Two silica sands differing by a factor of 10 in mean particle size (D_{50}) were used as the base material matrix for the specimens. This selection was driven by a desire to assess the suitability of MICP for creating synthetic rock specimens across a wide range of particle sizes, possibly beyond natural rock characteristics as this would allow the use of bespoke materials with exaggerated features in further testing programs.

The characteristics of both sands are reported in Table 1. The fine sand had a D_{50} of 0.18 mm, while the coarse sand D_{50} was 1.82 mm. The particle size distribution curves are shown in Fig. 2. The mineralogy and other characteristics of the sands were similar: both sands were uniform and had sub-rounded grains with medium sphericity. The coefficient of uniformity was 1.38 and 1.33 for the fine and coarse sands, respectively. The average grain size of the fine sand falls in the optimum range of grain sizes for bio-cementing and has been used widely (DeJong et al. 2006; Al Qabany et al. 2012) whilst according to Mitchell and Santamarina (2005), the coarse sand used in this study is not recommended for bio-cementation due to the large size of its pores (see Fig. 1).

Sand	Mineralogy	Grain Angularity	Average particle diameter (mm)	Coefficient of uniformity Cu	Coefficient of curvature Cc	Initial porosity
Fine	Quartz	Sub-rounded	0.18	1.38	0.89	0.38-0.42
Coarse	Quartz	Sub-rounded	1.82	1.33	1.05	0.33-0.37

Table 1. The characteristics of the two sands used in this study

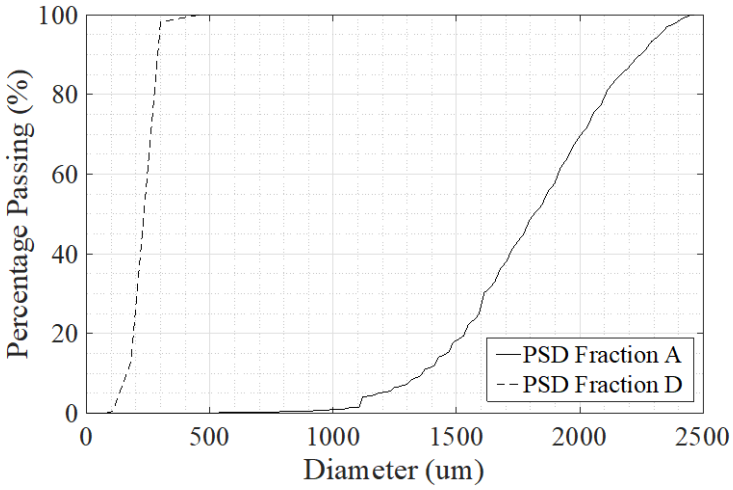

Fig. 2. Particle size distribution curves for fine and coarse sands

To create test specimens, the sand was placed in cylindrical molds of 70 mm diameter and 220 mm height and vibrated until the porosity of the fine sand was in the range of 0.38-0.42 and the porosity of the coarse sand was between 0.33-0.37.

The treatment was carried out in two phases: (1) 330 ml of bacteria solution (BS), equivalent to 1.1 the specimen pore volume, was injected only once at the beginning of the process and allowed to saturate the specimen for 24 hrs; (2) multiple injections of 330 ml of cementation solution (CS), each equivalent to 1.1 times the pore volume of the specimen, were then delivered at regular 24 hr intervals.

The number of injections of cementation solution depended on the desired final cementation level, defined as weight of calcium carbonate over the total weight of the sample, and the efficiency of the process in transforming available reactants into calcium carbonate, i.e. the ratio of calcium carbonate precipitating over calcium chloride introduced to the sand columns.

The theoretical number of injections was calculated as the total volume of cementation solution required for precipitation of the specified amount of desired cementation level (carbonate content) divided by the volume of one injection (330 ml), assuming that all reactants were converted into products. A preliminary testing program determined that the efficiency of the

process was around 80% and 60% in the fine and coarse sands, respectively. The number of injections needed to achieve a targeted cementation level was calculated based on these values: for example, if the theoretical number of injections to achieve a specific cementation level was 10, then the actual number of injections required to achieve the target would be 12 for the fine sand and 16 for the coarse sand.

Injection via gravity was selected, since it has been shown to result in uniform samples when compared to other methods (Mujah et al. 2017) and the grain size of the fine sand used in this study falls in the optimum range to inject with this technique. Filters were placed at the top and bottom boundaries to diffuse the flow evenly. A similar protocol was applied by Al Qabany et al. (2012) for smaller samples with 35.4 mm diameter. The experimental setup is illustrated in Fig. 3. With each new injection, the previous solution was allowed to drain out and at the same time, new solution was introduced to the specimen. Outward flow was stopped when 1.1 pore volume of solution had been collected at the outflow. The saturated specimen was allowed to rest for a 24 hr retention period for both bacteria and cementation solution injections. The overall MICP treatment process was completed once the pre-defined number of injections of chemical solution had been administered.

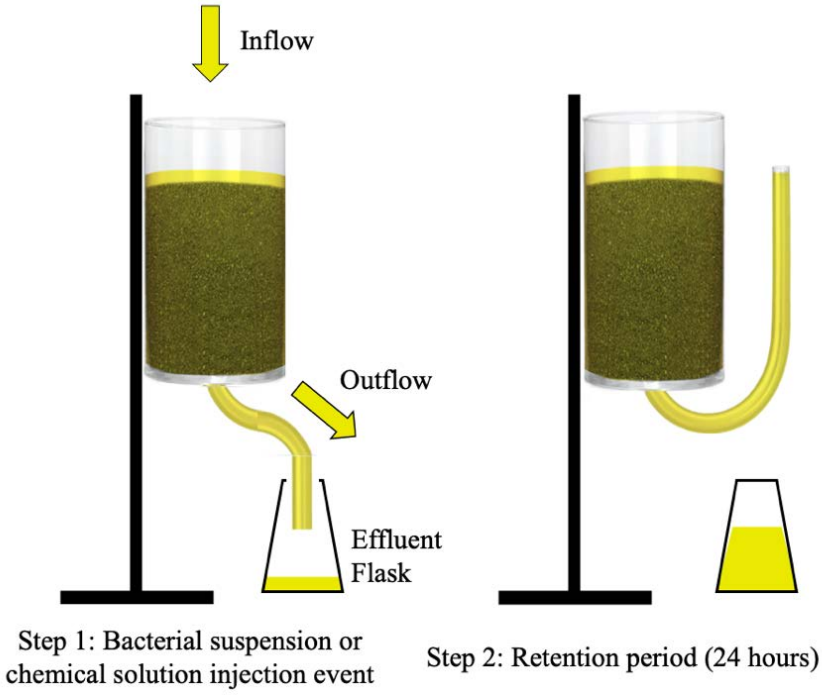

Fig. 3. Experimental setup - Stepwise injection via gravity: Step 1 – Injection; Step 2 - retention period.

At the end of the last retention period, specimens were extracted from the molds with care to minimise disturbance. About 10 mm were trimmed from the ends of the sand columns to eliminate potentially disturbed or uneven zones. The remaining portion was divided in two parts, one to provide a specimen with a final height of 150 mm to conform to the ASTM standard for unconfined compression testing, the other to be used for point load tests.

The only parameter allowed to vary across specimens was the number of injections, resulting in different cementation levels.

3.3. Experimental characterisation

The effectiveness of the proposed approach in producing consistent and controlled characteristics was evaluated through a series of tests. Uniformity, repeatability and efficiency were assessed for varying calcium carbonate contents. These metrics define how easy it is to produce specimens of a desired cementation level and, most importantly, the quality of those

specimens for the purpose of laboratory testing. Chemical efficiency, defined as the amount of reactants converted into products, was often used in previous studies to assess the effectiveness of the MICP process and is included in this study to compare the findings. The strength of the specimens at various cementation levels and porosities was measured with unconfined compressive strength and point load tests. Microscopy images were taken to understand the morphological differences in the bio-cemented material, which may explain strength variations.

3.3.1. Calcium carbonate Content

Calcium carbonate content was measured according to the procedure in ASTM D4373-14 (ASTM 2014). A 30 g dried and ground sample was treated with 30 mL of hydrochloric acid (HCl) of 2.5 M. Calcium carbonate ($CaCO_3$) is dissolved according to the reaction:

$$CaCO_{3(s)} + 2HCl_{(aq)} -> CaCl_{2(aq)} + CO_{2(g)} + H_2O_{(l)} \quad (1)$$

Carbon dioxide is released into a chamber (calcimeter) equipped with a pressure gauge. The pressure reading is translated into amount of carbon dioxide, allowing the amount of calcium carbonate to be calculated with the aid of the stoichiometry of the reaction. The degree of cementation (C_w) is expressed in this study as weight of calcium carbonate over the total weight of the sample tested (in percent).

3.3.2. Unconfined Compressive Strength and Point load tests

Unconfined compressive strength (UCS) and point load tests (I_s) were performed on oven dried specimens with varying levels of cementation. For the UCS tests, the samples were prepared and tested according to ASTM D7012-14e1 (ASTM 2004) and ASTM D2938:390-391 (ASTM 1995). The specimens in the axial compression tests had a 70 mm diameter and a 150 mm height. The loading of the samples was displacement-controlled with a rate of 1.14 mm/min.

Point load tests were conducted on core and lump specimens to assess the rock strength index

following ASTM D5731-16 (ASTM 1985). Care was taken in order to induce failure between the tenth and the sixtieth second of the test. The smallest dimension of the specimens in the lump tests was no less than 30 mm.

3.3.3. Final porosity

Porosity (n) is defined as:

$$n = 1 - \frac{\varrho}{G_s} \tag{2}$$

where ϱ is the bulk dry density and G_s is the specific gravity of the porous material. The final porosity was calculated using an equivalent specific gravity that takes into account the specific gravities of the individual minerals present based on the relative volume fraction. For a rock that consists of two minerals (Sharwood 1912):

$$G_s = \frac{W_{total}}{\frac{w_1}{G_{s1}} + \frac{w_2}{G_{s2}}} \tag{3}$$

where W_{total} is the total dry weight of the artificial material, w_1 and w_2 are the weight of quartz and calcium carbonate within the rock, respectively. G_{s1} and G_{s2} are the specific gravities the of quartz and calcium carbonate, equal to 2.65 and 2.71 respectively.

3.3.4. Microstructural Observations

Environmental scanning electron microscope (ESEM) images of MICP treated samples were taken to investigate the morphology and distribution of calcium carbonate crystals and their bonding network. The microscopy investigation was carried out with a PHILIPS XL30 scanning electron microscope. All MICP treated samples were dried at 100°C for 24h before conducting the microscopy analysis.

4. RESULTS & DISCUSSION

The effectiveness of the MICP process and the resulting mechanical properties were significantly affected by the particle size distribution of the matrix material. The same number

of injections resulted in different calcium carbonate concentration levels due to variations in chemical efficiency. Even when the concentration levels were similar, the resulting cemented material properties varied for different particle size distributions (PSDs). These effects are examined separately in this study since a single recipe was followed for both types of sands in order to eliminate any influence from bio-chemical factors.

4.1. Effectiveness of MICP in the fine and coarse sands

Three metrics were used to assess the ability of MICP to produce suitable specimens: chemical efficiency, repeatability, and uniformity. Chemical efficiency is defined as the amount of calcium carbonate in the final specimen (in mol/litre) relative to calcium chloride injected in mol/litre expressed in percentage. Calcium chloride was chosen over urea as it is the limiting factor in the reactions (the ratio of urea to calcium chloride is 1.5:1, therefore if all calcium chloride is consumed there is an additional 0.125 M urea left). Although the chemical efficiency is not directly related to the quality of the specimens, it is generally used to assess the effectiveness of the process in other works, which will be used for comparison with the results presented here. Repeatability, which is derived from chemical efficiency, accounts for the ability to produce similar outcomes starting from the same components and quantities through the same process and it is a more appropriate figure for the purposes of this research. Repeatability is assessed with plots of actual vs targeted cementation levels. Uniformity measures the spatial distribution of the cementing agent across the height of the specimens.

The three metrics were assessed against measurements of carbonate content at four to five points along the height of each specimen. Examples of cementation level profiles are reported in Fig. 4 for the fine and coarse sand specimens at a medium cementation level within the range targeted in this study. The calculations for chemical efficiency and repeatability were based on the average cementation level of the specimen, while the degree of uniformity was assessed based on the variance of the cementation level for each profile.

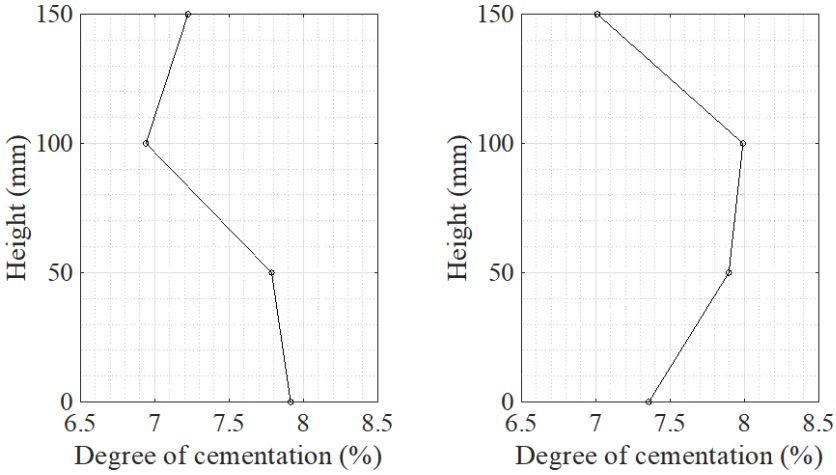

(a) **(b)**

Fig. 4. (a) Cementation level profile of fine sand and (b) Cementation level profile of coarse sand at an average cementation level of 7.5%

4.1.1. Chemical efficiency

The measured chemical efficiency is plotted against the degree of cementation for the fine and coarse sands in Fig. 5. The results include all samples developed for this study. The precipitation efficiencies of calcium carbonate of the coarse sand specimens are around 60% and almost constant at all cementation levels, although with some scatter. In contrast, the efficiencies of the MICP process in the fine sand specimens are about 80% at a cementation level of 4%, falling to 70% at higher degrees of cementation.

The lower chemical efficiency at high cementation levels can be explained by the heavy precipitation of calcium carbonate at the injection point, leading to clogging of the pores. This in turn, hindered further penetration of the cementation liquid into the sample. Although the system had low reaction rates due to lower urease activities, as the cementation level increased, the flow rate decreased, allowing more of the chemical solution to be consumed around the injection point. This portion of the specimens was eliminated and only the central 180-200 mm were used in the following studies.

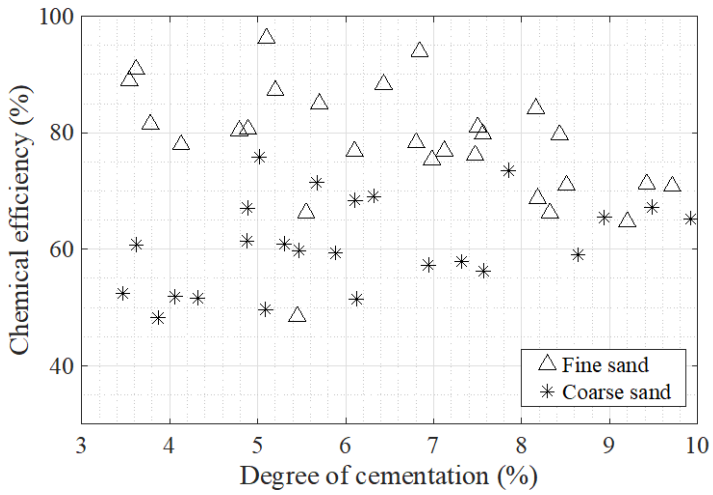

Fig. 5. Chemical efficiency at various cementation levels

Injections in the fine sand specimens showed lower chemical efficiency values compared to Al Qabany et al. (2012) who found that the chemical efficiency remained approximately constant with the degree of cementation at around 90% or above (for calcium chloride concentrations of 0.25 M). While the chemical recipe and the experimental protocol in the two works are similar, lower urease activity in this study, in conjunction with much longer retention times or even different surface conditions (chemical characteristics etc.) on host grains, may explain a reduction in the chemical efficiency. Achieving high cementation levels required a large number of injections of chemical solution, increasing the overall duration of the bio-treatment to 16 or even 20 days, and leading to substantial reduction in bacterial activity towards the end of the process (van Paassen 2009; Konstantinou 2020).

Although it was expected that the MICP process would have lower efficiency in sands with larger particle size, resulting in very lightly cemented samples, this was not the case in this study. The high density of the bacteria (optical density of 1.5- 2.0) increased the probability of microbes attaching to the particles and the long retention time between the bacteria injection and the first cementation solution injection improved the settlement of bacteria, therefore

increasing efficiency. The efficiency of injection in the coarse sand specimens was still lower compared to that of the fine sand specimens as, inevitably, more bacteria were flushed out of the specimens due to the higher flow rate (20-30 ml/min) during the first cementation solution injection when the suspension liquid was removed (Liu et al. 2019; Wang et al. 2019a). Measurements of the optical density were taken in approximately every 60 mL of effluent after the first injection. For coarse sand, the OD_{600} of the first 60 mL was around 0.9 and increased to 1.3 in later stages, before finally decreasing again towards the end. The OD_{600} of the effluent for fine sands was lower throughout the process at 0.7-1.

Fig. 6 shows results of this study against the findings by Rebata-Landa (2007) for a target cementation of approximately 5% for varying particle sizes. The solid line and curve represent the findings of Rebata-Landa (2007). The author injected the same amount of chemical solution in soils with varying grain sizes and showed that no cementation takes place for particle size less than 1 μm and then the precipitation level increases linearly up to 100 μm. Above the threshold of 100 μm, the cementation level decreases substantially. The figure includes the range of average cementation level for fine and coarse sand specimens with targeted cementation of 5% (triangles). The fit provided by Rebata-Landa (2007), was shifted upwards to match the experimental data of this work (dashed curve). While the fine sand specimens in this study showed similar results, the coarse sand specimens performed better than predicted in Rebata-Landa's study demonstrating good chemical efficiency, and thus good repeatability. Recent experiments on microfluidic chips (Wang et al. 2019a, 2019b) have proven that bacteria form aggregates as soon as the cementation solution is injected, with aggregates increasing in size with larger optical density. The MICP procedure in this study adopted optical densities in the upper range studied by Wang et al. (2019a) possibly resulting in larger aggregates which are more likely to settle within the porous medium instead of being flushed out of the specimen, leading to overall higher chemical efficiency. The higher efficiency found in this study extends

the micro-fluidics findings by Wang et al. (2019a) to actual soils.

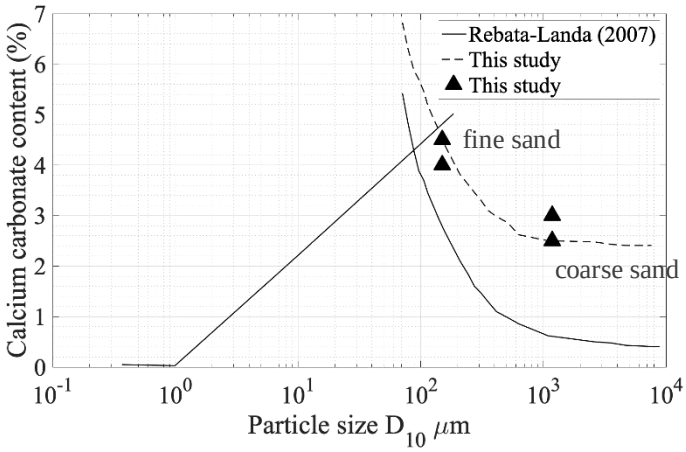

Fig. 6. $CaCO_3$ content and models as a function of grain size (after Rebata-Landa (2007))

4.1.2. Repeatability

One of the objectives of this work was to generate artificially cemented sands with similar carbonate characteristics but with varying cementation levels in a repeatable manner. Fig. 7 presents the averaged degree of cementation of both fine and coarse sand specimens with respect to the number of injections. In both cases, the relationship is linear, demonstrating the success of the design of the MICP procedure as the number of injections largely controls the amount of cementation. Clearly, for the same number of injections, larger amounts of carbonate precipitate in fine sands than in coarse sands. However, at higher injection numbers the difference between the precipitating cement in fine and coarse sands becomes smaller.

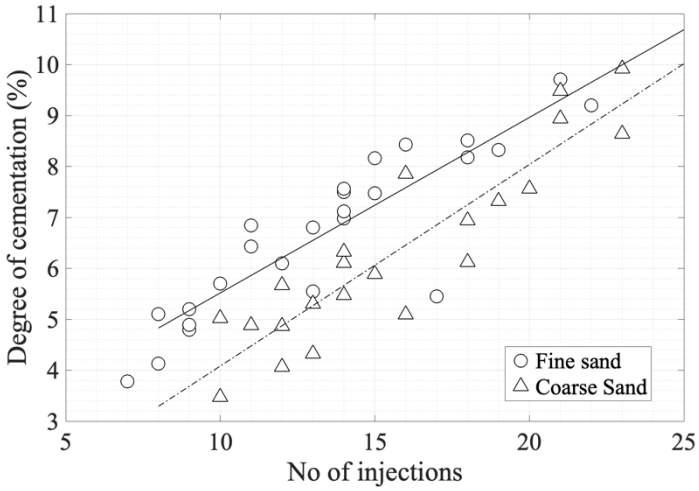

Fig. 7. Number of injections and the degree of cementation

Fig. 8 shows the average degree of cementation of each specimen, derived by averaging the measurements of calcium carbonate across the height of each sample. In the fine sand with 5-7% target cementation, the achievable values are similar to the targeted ones, as the data points are concentrated around the 1:1 line, while over 7% the achievable values are lower. In the coarse sand, the achievable cementation levels are more scattered and the averages for each cementation level are lower than the targeted ones. The results confirm generally good repeatability for the fine sand and a lower degree for the coarse sand.

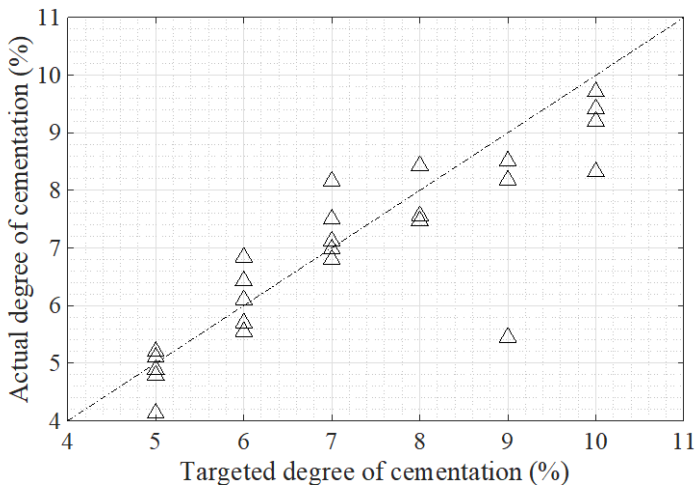

(a)

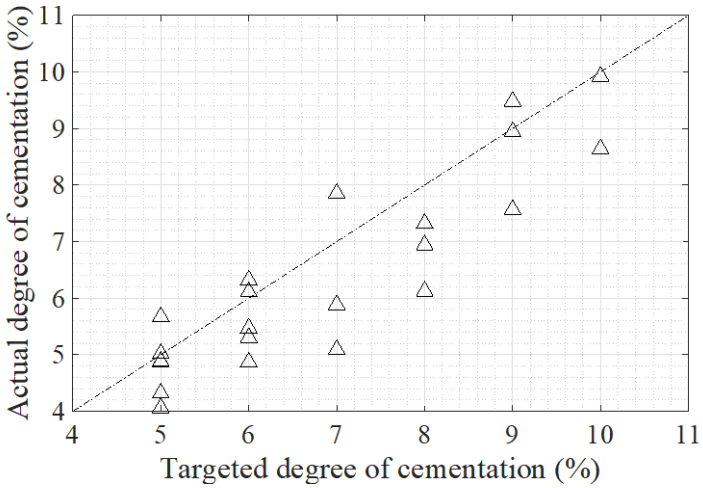

(b)

Fig. 8. Actual vs targeted degree of cementation for (a) fine and (b) coarse sands.

4.1.3. Uniformity

As shown in Fig. 9, the variance in uniformity of cementation measurements declines as the cementation level increases, indicating more uniform samples at the highest range of about 10% (g of calcium carbonate/ g of specimen). The carbonate precipitation in the fine sand specimens is relatively uniform above 5% cementation, while similar variability is observed for the coarse sand at slightly higher cementation levels (6%-10%). No particular trend was observed in the precipitation profiles across the height of each sample. A possible explanation for observed trends in variance when the cement content increases is that, once the easily accessible pores are filled with cement, the cementation solution in a subsequent injection is forced to flow in what were originally less permeable parts of the sand. The coarse sand samples were uniformly cemented along the height because the high injection rates, and the longer retention times (24 hours is towards the longer intervals being used previously) in conjunction with the low bacteria activity, allowed the reaction to take place almost at the same time along the height of the sample. For the fine sand specimens, although the injection rate was lower, this was compensated by the low bacterial activity, which resulted in low urease

conversion rates.

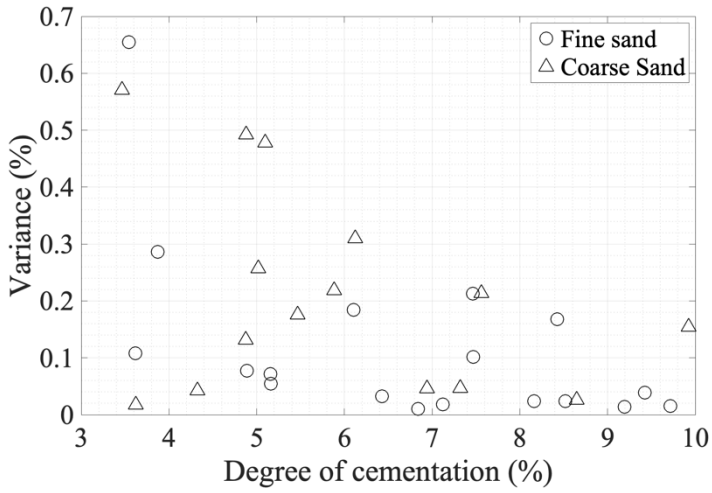

Fig. 9. Variance of uniformity profiles

Since the coarse sand specimens had higher flow rates, a more uniform cementation distribution would be expected. This trend was indeed observed by Cheng and Cord-Ruwisch (2014), on sands falling in the optimum compatibility region (Mitchell and Santamarina 2005). However, it is not the case for the coarse sand used in this study. The literature review has shown conflicting results between different authors on uniformity versus cementation level. Previous studies including uniformity measurements (Feng and Montoya 2015; Lin et al. 2015) did not use injection via gravity for delivering the solutions. Therefore, at least some of the difference in trends between the results of this study and those of previous works may be attributed to the injection method.

The highest variation in calcium carbonate content within a specimen was in the range between 1.5 and 2.0 % by weight, whilst the most uniform specimens had cementation level varying by only 0.1 to 0.2 % by weight. Most of the previous studies in fine sands have shown differences larger than 1.5% in calcium carbonate content within each sample (Dawoud 2015; Feng and Montoya 2015; Cui et al. 2017). Very few studies provide uniformity profiles of different bio-sands with particle sizes produced through the same MICP procedure. Limited results presented

by Lin et al. (2015) suggest that medium-fine sands (average particle diameter of 0.71 mm) tend to produce less uniformly cemented products compared to the fine ones. The very coarse bio-cemented sands (average particle diameter of 1.6 mm) obtained by Mahawish et al. (2018) also show limited success in controlling the MICP process when large particles are used, since the average variation between the measurements of calcium carbonate content within each sample are about 3 % by weight. The conflicting observations can be explained by the very different MICP procedure followed by Mahawish et al. (2018) compared to the one in the present study. The review of these previous studies highlights the challenge of comparing outcomes of different MICP processes.

4.1.4. Relation between the three metrics

There is a trade-off between chemical efficiency and the degree of uniformity as the chemical efficiency and variance in carbonate content decline with the increase of cementation. This means that, for specimens generated with the bio-chemical and injection methods selected in this study, a more cemented specimen is more uniform, but more difficult to obtain because the efficiency decreases when cementation is higher. The long injection intervals of 24 hours extended the overall duration of the injection phase. When a higher cement content was targeted, a decline in bacterial activity was observed towards the end of the injection phase due to the larger number of injections and, therefore, the extended amount of time was needed to achieve the targeted cementation (van Paassen, 2009).

4.2. Effects of degree of cementation and porosity on strength

UCS and point load index tests were performed to examine the correlation between the degree of cementation and the strength of the samples. Examples of the stress strain curves obtained for the fine and coarse MICP-treated sands at low (5.5%) and high (10%) cementation levels are presented in Fig. 10 (a) and (b), respectively.

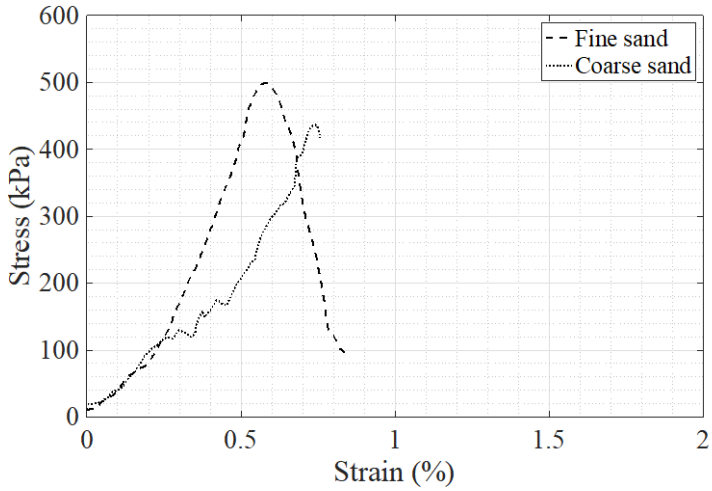

(a)

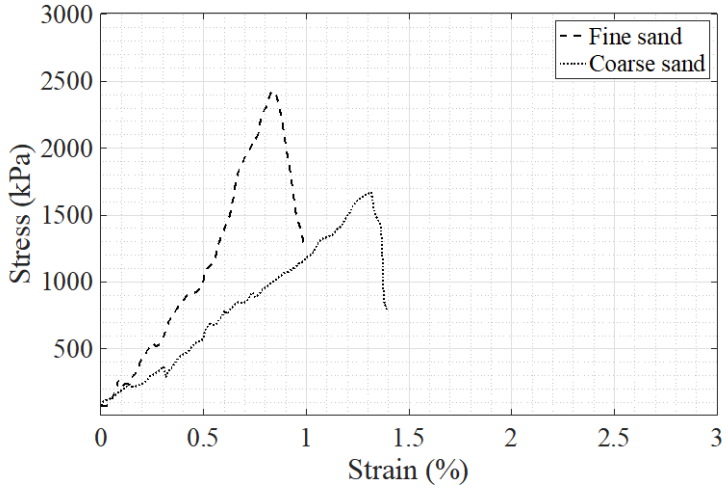

(b)

Fig. 10. Stress strain curves for both fine and coarse MICP-treated sands at (a) low and (b) high degrees of cementation

The strength increases substantially as the cementation level changes from 5% to 10%, from 500 kPa to about 2500 kPa and from 450 kPa to 1600 kPa for the fine and coarse sands, respectively. These values fall within the range of measured strengths of natural soft sandstones reported in the literature. The sharp peak, immediately followed by a dramatic decrease in the strength, indicates brittle failure, which occurred at less than 2% strain. The stress-strain curve of MICP-treated coarse sand specimens shows fluctuations due to the appreciable dislocation

when crushing of the bonds causes closure of the voids. Between 5% and 10% cementation, the specimens show a characteristic axial splitting mode. These observations are also consistent with previous MICP work by Cheng et al. (2013) and van Paassen et al. (2010). Visual inspection revealed that the weakest specimens tended to disaggregate at grain scale with the particles of the coarse sand, especially, detaching from the failure surface.

Five coarse sand specimens with low to medium cementation levels failed as soon as the initial load was applied as they were weaker at one of the two ends, adjacent to the top or bottom pedestal. They were treated as having null strength and were removed from the subsequent plots. The samples' uniformity could not be assessed as the original location of the grains could not be identified.

Both sands show a substantial increase in strength when the cementation increases (Fig. 11 (a)), as found by many authors (Al Qabany and Soga 2013; Feng and Montoya 2015; Lin et al. 2015). The sand matrix is originally cohesionless and unstable structures are formed at lower calcium carbonate contents. The gain in strength is relatively small at lower cementations, but it becomes more pronounced at higher cementation levels and especially in the fine sand above 7% cementation. At a cementation level of 3%, the ratio of the UCS of the coarse sand to the UCS of the fine sand is at about 90%, as shown in Fig. 11 (b). The ratio decreases to about 60% at a cementation level of 10%. An exponential curve provided the best fit for both fine and coarse sands, as shown in Table 2.

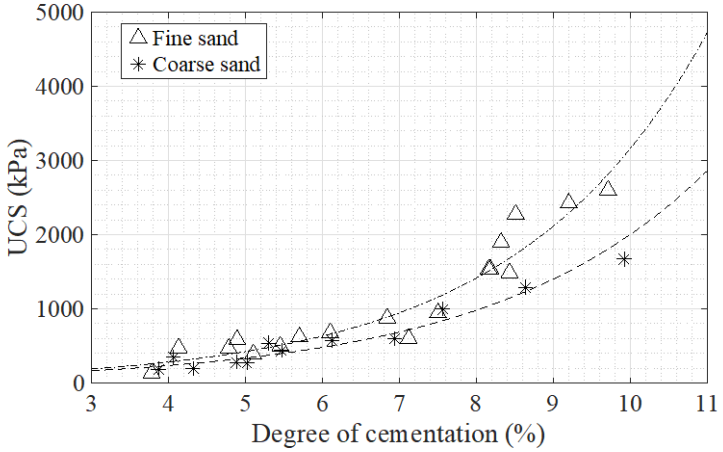

(a)

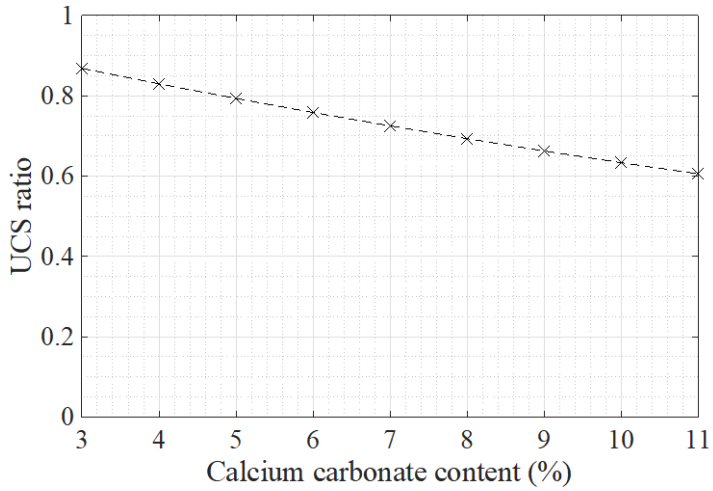

(b)

Fig. 11. (a) UCS results with various degrees of cementation for MICP-treated fine and coarse sand specimens (b) UCS of coarse sands over the UCS of fine sands with respect to cementation level

Type of correlation	Type of sand	Expression	R^2
UCS = f(cementation level)	Fine	$\mathrm{UCS} = 56.911 * \exp(0.4018 * C_w)$	$R^2 = 0.87901$
	Coarse	$\mathrm{UCS} = 56.544 * \exp(0.3568 * C_w)$	$R^2 = 0.90103$
Is = f(cementation level)	Fine	$\mathrm{Is} = 21.385 * \exp(0.3979 * C_w)$	$R^2 = 0.7709$
	Coarse	$\mathrm{Is} = 18.44 * \exp(0.3337 * C_w)$	$R^2 = 0.8231$
UCS = f(porosity)	Fine	$\mathrm{UCS} = 0.0888 * n^{-8.715}$	$R^2 = 0.6866$
	Coarse	$\mathrm{UCS} = 0.0053 * n^{-9.526}$	$R^2 = 0.8353$

Table 2. Curve fitting for UCS with respect to cementation level and porosity and Is with respect to cementation level

The strength was also assessed by point load index tests. The measurements are plotted with respect to the degree of cementation in Fig. 12 (a). The coarse sand samples with less than 4% degree of cementation were very weak, making this test unsuitable. Although the results are more scattered compared to the UCS results, an exponential regression curve provided a best fit for both types of sands (Table 2). The exponent values are 0.3979 and 0.3337 for the fine and coarse sands, respectively, which are similar to those obtained in the UCS tests. At lower cementations the ratio of the point load strengths of the coarse sand over that of the fine sand is about 71% and it reduces to 50% at higher concentration levels, as shown in Fig. 12 (b).

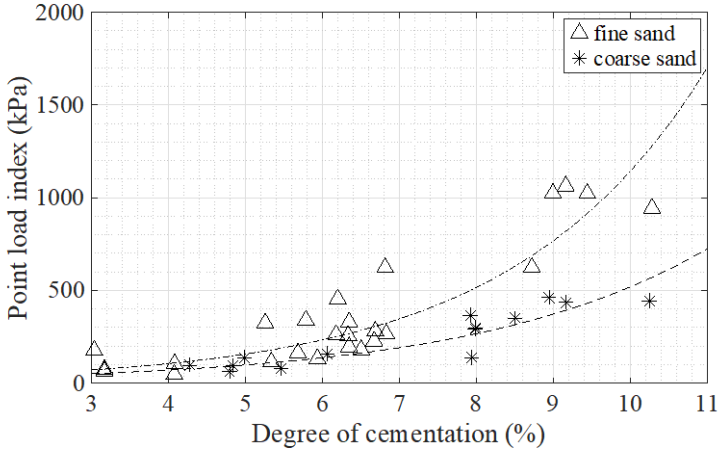

(a)

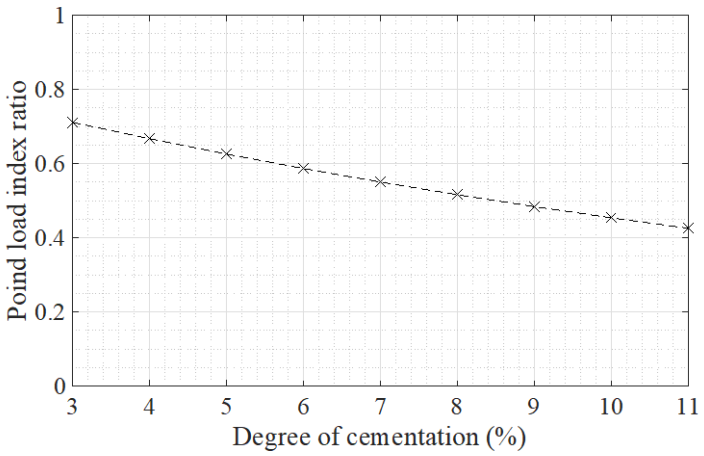

(b)

Fig. 12. (a) Point load index results with respect to various degrees of cementation for fine sands and coarse sands (b) Point load index of coarse sands over the point load index of fine sands with respect to cementation level

Coarser particles form fabrics with larger pores, but overall smaller porosity, because they cannot achieve stable and very open arrangements. If particles are spaced too far apart the structure quickly collapses under small solicitations. Finer particles are able to form more open stable arrangements with higher porosity, but smaller void sizes. The larger number of particles in the same volume also results in larger surface area and more contact points available for calcium carbonate deposition. Fig. 13 shows that the final porosity of the MICP treated fine

sand specimens falls in the range of 0.3-0.4 and the final porosity of the MICP treated coarse sand specimens falls in the range of 0.25-0.35. A power function provided best fits for both types of sands (highest R-squared values). As seen in Table 2, unconfined compressive strength is higher when the final porosity is lower; as porosity decreases, a higher proportion of the voids is filled with calcium carbonate and a further reduction of porosity causes higher gain in strength. This trend is more evident in the fine sand where the initial void sizes are smaller and more readily occluded.

In the common porosity range (0.3-0.35), the UCS of fine sand is four to five times that of the coarse sands, bracketing the range of achievable strengths and porosities. By varying the grain size, and possibly the width of the particle size distribution, it is possible to achieve different combinations within the boundaries shown. Plumb (1994) reported an empirical relationship to correlate soft sandstones' strength with porosity in a power form and specified an upper boundary. As shown later, both the fine and coarse sand specimens' data points fall below the upper strength limit, in the region of the plot towards the higher porosity range measured for natural materials.

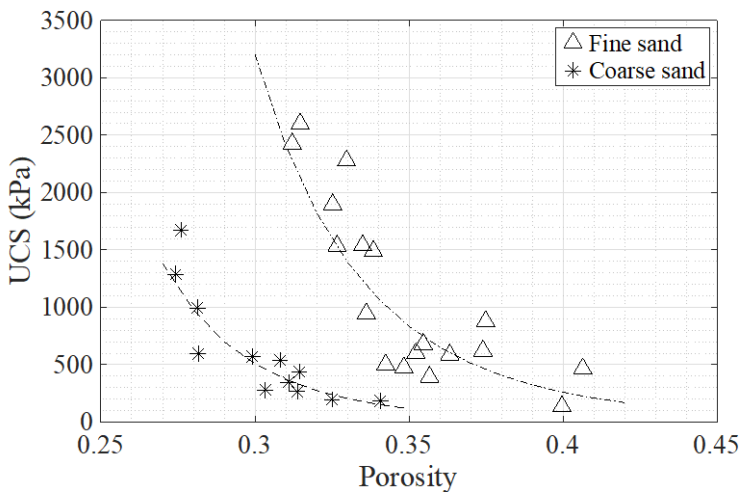

Fig. 13. UCS results with respect to porosity

The increase in strength is a function of both the final porosity and cementation level, as seen

in Figs. 12 and 13. Consoli et al. (2010) utilised a power function to express UCS as a function of the ratio of the volumetric cement content, defined as volume of calcium carbonate over the total volume of the sample (C), and porosity of the specimen, which accounts for the conjugate effects of these variables on the strength of the samples (Consoli et al. 2007, 2011). The porosity over the volumetric cement ratio is often adjusted by an exponent ξ which is selected across a range of possible values to provide the best fit.

$$UCS = f\left(\frac{porosity}{volumetric\ cement\ ratio^{\xi}}\right) = f\left(\frac{n}{C^{\xi}}\right) \tag{4}$$

The UCS values obtained from the tests are plotted against this ratio (Fig. 14). The coefficient ξ giving the best fit for the fine sand is 0.97 and that for the coarse sand is 1. Both coefficients are very close to 1, which, according to Rios et al. (2013), indicate that the two sands have the same mineralogy and similar particle shape, as well as being uniform.

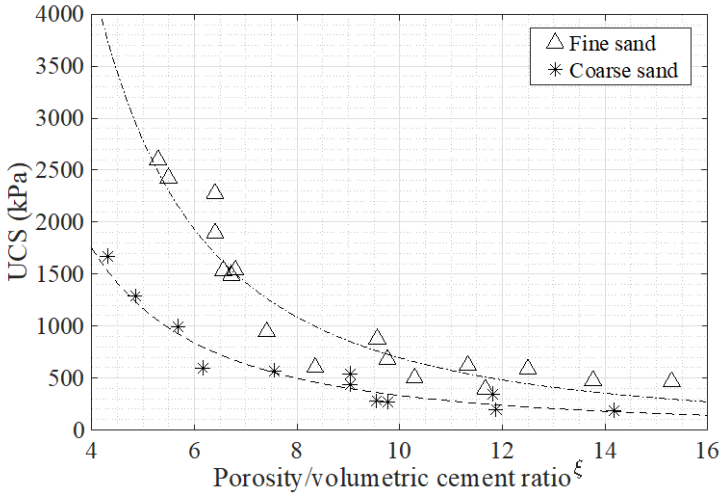

Fig. 14. UCS Vs. **porosity/ (volumetric cement ratio)$^{\xi}$** ratio: Power fit for coarse and fine MICP-treated sand specimens

The successful use of MICP to generate specimens using base materials with two very different grain sizes established specific combinations of strength and porosity. This initial work indicates that a similar approach can be used to treat materials with intermediate grain sizes or wider PSD.

4.3. Comparison of the properties of artificial specimens with natural weak sandstones

UCS is the most typical property measured when assessing the behaviour of rock, however, point load index tests are easier to conduct. The values for the ratio of UCS over I_s in this study were around 2.8 for fine sands and 3.3-3.9 for coarse sands, below the range of 6.6 to 30 reported in the literature for sedimentary and soft rocks (Rabat et al. 2020).

The strength of the artificial specimens in this study varied between 200 and 3000 kPa, falling in the range for very weak and extremely weak sandstones (ISRM 1981). UCS reported in the literature for a number of sandstones is collected in Table 3, demonstrating the great variability in natural materials from the same formations. Wide ranges of porosity (0.2-0.4) are also reported for this group of soft rocks, characterized by values that are generally higher than the ones reported for stronger sandstones associated with porosity of less than 0.1. In this study porosity fell in the interval 0.26 to 0.42 within the same wide range exhibited by the very weak natural carbonate cemented sandstones. Fig.15 presents pairs of UCS and porosities values found in literature, along with the trends identified for fine and coarse sands in Fig. 13, bracketing the grey area highlighting achievable strengths and porosities. A large portion of pairs reported in literature fall in the region of achievable strengths.

Name/Type of sandstone	UCS (kPa)	Porosity	Reference(s)
Waterberg	3338	0.2	Mohlala (2016)
Shihti and Kweichulin Formations	880- 3200	0.24-0.27	Chen and Hu (2003)
Kidderminster	440-2070	0.31	Dobereiner (1984); Freitas and Dobereiner (1986)
Bauru	850-5100	0.27-0.35	Dobereiner (1984); Freitas and Dobereiner (1986)
Lahti	3600	0.28	Dobereiner (1984); Freitas and Dobereiner (1986)
Coina Sand	500	0.32	Freitas and Dobereiner (1986)
Castanheira sand	100	0.35	Freitas and Dobereiner (1986)
Ferrel sand	500	0.33	Dobereiner (1984)
Entrada sandstone in Utah, USA	1080-1980	0.27	Larsen (2015)
DV sandstone	1640-3720		D. S. Agustawijaya (2007)
Saltwash South	1900-2070	0.3-0.31	Ispas et al. (2012); Pradhan et al. (2014)
Pleistocene sandstone, shale	200-1200		Huang and Pan (1999)
Pleistocene Toukoshan Formation	100-1300		Ku et al. (2008)
Antler sandstone	1200	0.35	Krishnan et al. (1998)
Nottingham Castle Sandstone Formation	516-1530	0.307	Sattler and Paraskevopoulou (2019)
Dubai weak calcareous sandstones	500-5000		Elhakim (2015)
Calcarenite from the site of the off-shore gas platform of North Rankin in Western Australia	500-2000		Cuccovillo and Coop (1997)
Silica sandstone from the Lower Greensand series of Kent in England.	600		Cuccovillo and Coop (1997)
Cemented sands from Asunción	100-5000	0.27	Kanji (2014)
Terciary	800-2000	0.36-0.37	Kanji (2014)
Aztec sandstone	1000-2000	0.26	Haimson and Lee (2004)

Table 3. Unconfined compressive strength (UCS) and porosities for soft rocks reported in previous studies.

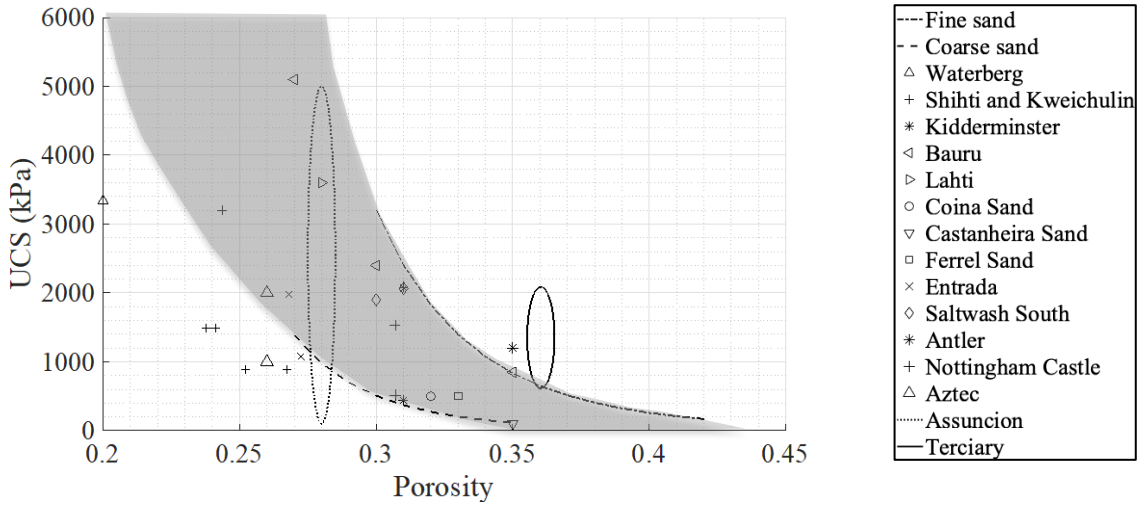

Fig. 15. UCS with respect to porosity with values reported in literature (Table 3) and the results of this study

4.4. Microstructural analysis

The microstructure of natural sandstones is also a key to their characterisation. The predominant matrix mineral of weakly cemented sandstones is quartz and the cement is often carbonate (siliceous cement, calcium carbonate, or calcareous cement) or clay minerals (Krynine and Judd 1957; Fjar et al. 2008). The degree of binding action depends on the amount and type of cementing agent (Sitar et al. 1980) whilst the behaviour of most cemented sandstones appears to be quite similar, regardless of the particular cementing agent (Collins and Sitar 2009).

The data from the MICP specimens show that the cementation level cannot fully describe the variation in strength across the two types of sands; the fine sands have higher strengths compared to the coarse sands for a given degree of cementation and porosity (Fig. 12). Strength is not only affected by the amount of cementation, but also depends on the initial spatial configuration of the grains and the microstructural characteristics of the cementation material within the original sand structure.

The MICP procedure (bacterial optical density, activity, concentration of chemicals, flow rate)

largely controls the delivery and distribution of bacteria within the soil, as well as the speed of the reactions. The calcite distribution within the granular network, in turn, depends on the position of the microbes relative to the grains (at pore throats or against grain surface asperities) and the matrix configuration. These parameters, therefore, define the cement precipitation patterns relative to the porous medium.

Given that the MICP procedure is identical for both types of sand, it is reasonable to expect similar calcite crystal characteristics (shapes and sizes) at a given cementation level. However, the location and amount of calcite crystals are expected to be highly affected by the initial configuration of the granular fabric and the voids sizes. The larger the voids are, the lower the probability of a cement crystal forming at a pore throat. In the case of coarse sands, the voids' size is significantly larger than the expected calcite crystals' size due to the low chemical solution concentration, whilst in fine sands the voids are smaller and comparable to the calcite crystals' size.

The particle size also defines the total number of interparticle contacts in a given volume:

$$N_c \sim \left(\frac{1}{R^3}\right) \tag{5}$$

where N_c is the particle contact points number and R is the particle radius (Ismail et al. 2002, Gray, 1968).

The fine sand used in the present paper has 1000 times more contact points between the particles compared to the coarse sand, when all the other factors (grain shape and surface characteristics, sorting etc.) are assumed to be equal or negligible. It is therefore likely that carbonate crystals will land at contact points in the fine sand since these interparticle contact points are much higher in number compared to the coarse sand for a given volume.

Fine sand have an advantage in strength gain since cementation at particle-to-particle contacts acts as 'bridge' for the transmission of stresses acting on the granular skeleton, whereas

deposition of calcite on the faces of grains has a much smaller effect on strength.

The precipitation patterns (size and distribution of calcite crystals within the granular matrix) were evaluated with the aid of ESEM images of materials at low and high cementation levels (Fig. 16). The images were all taken with a magnification of 315X at a spatial resolution of 100 µm to allow a clear view of the relative position of the calcium carbonate crystals with respect to the grains and for comparisons of the absolute sizes of the crystals between the two sands. The first image from each category (cementation level and type of sand) uses arrows to indicate grains and circles to indicate calcite crystals. In the fine sand with low concentrations of calcium carbonate, crystals are observed mainly at particle-to-particle contacts with limited deposition at non-effective locations (Fig. 16 (a)-(b)). However, only a small portion of the intergranular contacts are filled with cement, resulting in low strength gain (Fig 17(a)). Failure occurs through the path of uncemented contact points, representing the weakest points. As more calcite crystals are deposited, they also bond a larger portion of effective locations, resulting in the faster strength increase. For very high concentrations (Fig. 16 (c)-(d) and Fig. 17 (b)) the crystals fill the available voids, such that the sand grains act as rigid inclusions in a soft matrix of cement and macropores (Saidi et al. 2003).

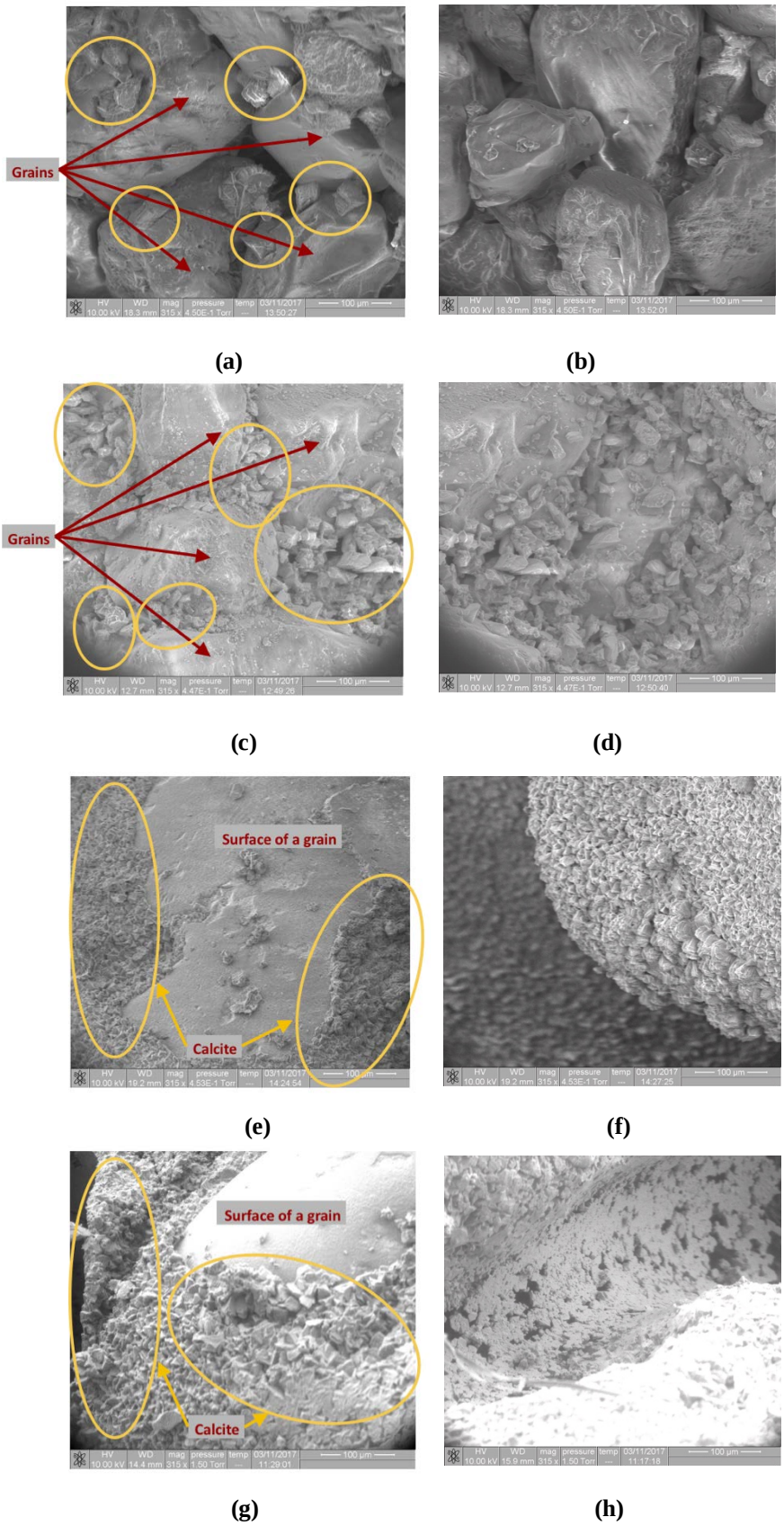

Fig. 16 . SEM images for (a)-(b) lightly and (c)-(d) heavily cemented fine sands (e)-(f) lightly and (g)-(h) heavily cemented coarse sands

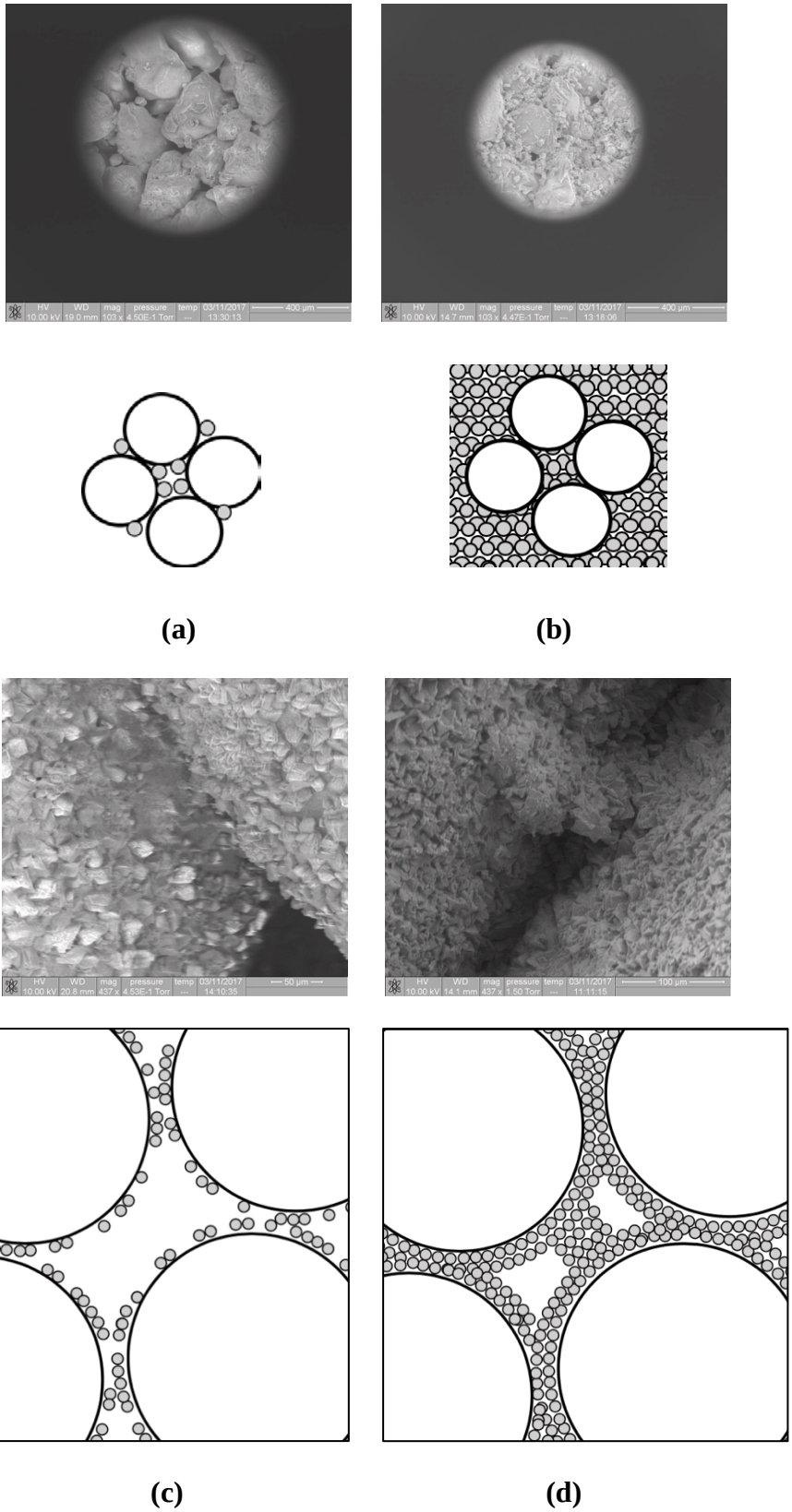

Fig. 17. SEM images for (a) lightly cemented fine sand, (c) lightly cemented coarse sand, (b) heavily cemented fine sand (d) heavily cemented coarse sand

The microstructure of the coarse sand differs from that of the fine sand. Calcite accumulates on the surface of the grains (surface coating), as well as on the effective locations (Fig. 16 (e)-(h)). The calcite crystals have similar shape and size to the ones observed in the case of the fine sand; however, they form clusters indicating that calcite gradually precipitates within the matrix (Terzis and Laloui 2019).

The particle contacts enhanced by MICP-cementation account for a smaller percentage of the deposited calcite resulting in lower strength gain (Fig 16 (a)). At higher cementation levels, the strength increases because more cement accumulates on the surface of particles and on particle-to-particle contacts. Given that the chemical efficiency is low in the coarse sand, it is not clear whether the MICP method adopted here would allow for the coarse sand to reach a state similar to the heavily cemented fine sands (all pores filled with calcite) and higher concentrations of calcite may have to be used to produce larger calcium carbonate crystals.

The cemented fine sands can develop higher strength because of the higher number of contact points and the more effective calcite distribution relative to the grains. Initial porosity is, therefore, critical in the coarse sands, as higher relative density provides more interparticle contacts and thus more effective locations for cementation, resulting in higher strengths. Results by Al Qabany and Soga (2013), suggest that higher concentrations of calcium chloride in the chemical solution during the injection phase could result in larger calcite crystals, which could potentially provide more effective bonding in coarse sands. The controlled and targeted cementation offered by the MICP procedure makes it a possible tool to develop artificial sandstone with consistent characteristics that can be customized by changing the formation process. The results also provide a potential approach to address the issue of uniform cementation in field applications of MICP, especially with coarser materials, by carefully calibrating bacterial urease activity, in conjunction with chemical concentrations in the cementing solution, and injection rates to balance speed of the reaction with flow rates.

5. CONCLUSIONS

The proposed MICP strategy reliably delivered artificial carbonate cemented sand specimens for laboratory testing purposes with consistent and controlled mechanical properties. Although the coarse sand with mean particle size of 1.82 mm is not considered an ideal candidate for MICP, the process presented in this paper was able to successfully produce cemented specimens with a good degree of uniformity and repeatability, especially at higher cementation levels. This outcome, in particular, provides a promising approach for other applications of MICP, including field ones, involving coarser materials. The key to obtaining uniform and repeatable products, especially in the coarser sand, was slow MICP reactions, due to lower concentration of the cementation solution, which allowed full permeation through the specimens. Long retention times, then, were required to ensure a high percentage of the cementation solution was transformed into calcium carbonate.

The strength increase of both sands could be controlled by targeting the appropriate degree of cementation through the number of injections. The identical treatment ensured consistency in size and shape of calcium carbonate crystals for all specimens, with only the amount of cementation changing between specimens. Strength increased exponentially with degree of cementation for both types of sands, with a more pronounced gain in the fine sand than in the coarse sand. This difference in strength cannot be explained solely by the cementation level, as the size of the host grains and void spaces significantly affect the distribution, and therefore the effectiveness, of the calcium carbonate. The microstructural images of the fine sand specimens show that a few small calcium carbonate crystals are sufficient to cement particle-to-particle contacts, whereas images of the coarse sand specimens show calcium carbonate deposition on both the surface of the grain and the contact points between the particles, requiring a larger amount of cementation to produce a comparable increase in strength.

The successful use of MICP to generate specimens using base materials with two very different

grain sizes established that more combinations of strength and porosity could be obtained using intermediate grain sizes, or PSDs, to meet the requirement of laboratory testing programs

The findings of this study can be extended to other potential applications of MICP, especially when coarser materials are involved.

6. ACKNOWLEDGEMENTS

This work has been carried out at the Department of Engineering at the University of Cambridge. We thank Chris Knight and the Department of Engineering technical staff for their help.

7. FUNDING

The authors would like to acknowledge the funding and technical support from BP through the BP International Centre for Advanced Materials (BP-ICAM) which made this research possible.

8. REFERENCES

Agustawijaya DS. The Uniaxial Compressive Strength of Soft Rock. Civ Eng Dimens [Internet]. 2007;9(1):9–14. Available from: http://puslit2.petra.ac.id/ejournal/index.php/civ/article/view/16584

ASTM. Standard Test Method for Determination of the Point Load Strength Index of Rock 1. Rock Mech. 1985;22(2):1–9.

ASTM. Standard test method of unconfined compressive strength of intact rock core specimens. In: 1995 Annual Book of ASTM standards. 1995. p. D 2938:270-271.

ASTM. Compressive Strength and Elastic Moduli of Intact Rock Core Specimens under Varying States of Stress and Temperatures. Stress Int J Biol Stress. 2004;4–11.

ASTM. Standard Test Method for Rapid Determination of Carbonate Content of Soils.

ASTM Int. 2014;1–5.

Bella G, Barbero M, Barpi F, Borri-Brunetto M, Peila D. An innovative bio-engineering retaining structure for supporting unstable soil. J Rock Mech Geotech Eng [Internet]. 2017;9(2):247–59. Available from: http://dx.doi.org/10.1016/j.jrmge.2016.12.002

Castro-Alonso MJ, Montañez-Hernandez LE, Sanchez-Muñoz MA, Macias Franco MR, Narayanasamy R, Balagurusamy N. Microbially induced calcium carbonate precipitation (MICP) and its potential in bioconcrete: Microbiological and molecular concepts. Front Mater. 2019;6:1–15.

Chen H, Hu ZY. Some factors affecting the uniaxial strength of weak sandstones. Bull Eng Geol Environ. 2003;62(4):323–32.

Cheng L, Cord-Ruwisch R. Upscaling Effects of Soil Improvement by Microbially Induced Calcite Precipitation by Surface Percolation. Geomicrobiol J. 2014;31(5):396–406.

Cheng L, Cord-Ruwisch R, Shahin M a. Cementation of sand soil by microbially induced calcite precipitation at various degrees of saturation. Can Geotech J [Internet]. 2013;50(1):81–90. Available from: http://www.nrcresearchpress.com/doi/abs/10.1139/cgj-2012-0023#.UUqWRRfvt8E

Cheng L, Shahin MA, Chu J. Soil bio-cementation using a new one-phase low-pH injection method. Acta Geotech [Internet]. 2019;14(3):615–26. Available from: https://doi.org/10.1007/s11440-018-0738-2

Cheng L, Shahin MA, Cord-Ruwisch R. Soil Stabilisation by Microbial-Induced Calcite Precipitation (MICP): Investigation into Some Physical and Environmental Aspects. 7th Int Congr Environ Geotech [Internet]. 2014;64(12):1105–12. Available from: http://hdl.handle.net/20.500.11937/37802

Cheng L, Shahin MA, Mujah D. Influence of Key Environmental Conditions on Microbially

Induced Cementation for Soil Stabilization. J Geotech Geoenvironmental Eng [Internet]. 2017;143(1):04016083. Available from: http://ascelibrary.org/doi/10.1061/%28ASCE%29GT.1943-5606.0001586

Collins BD, Sitar N. Geotechnical Properties of Cemented Sands in Steep Slopes. J Geotech Geoenvironmental Eng. 2009;135:1359–66.

Consoli NC, da Fonseca AV, Cruz RC, Silva SR. Voids/Cement Ratio Controlling Tensile Strength of Cement-Treated Soils. J Geotech Geoenvironmental Eng [Internet]. 2011;137(11):1126–31. Available from: http://ascelibrary.org/doi/abs/10.1061/(ASCE)GT.1943-5606.0000524

Consoli NC, Foppa D, Festugato L, Heineck KS. Key Parameters for Strength Control of Artificially Cemented Soils. J Geotech Geoenvironmental Eng [Internet]. 2007;133(2):197–205. Available from: http://ascelibrary.org/doi/10.1061/%28ASCE%291090-0241%282007%29133%3A2%28197%29

Consoli NC, Moraes RR de, Floss MF, Festugato L. Parameters Controlling Tensile and Compressive Strength of Fiber-Reinforced Cemented Soil. J Mater Civ Eng. 2010;136(5):759–63.

Cuccovillo T, Coop MR. Yielding and pre-failure deformation of structured sands. Géotechnique. 1997;47(3):491–508.

Cui MJ, Zheng JJ, Zhang RJ, Lai HJ, Zhang J. Influence of cementation level on the strength behaviour of bio-cemented sand. Acta Geotech. 2017;12(5):971–86.

Dadda A, Geindreau C, Emeriault F, Rolland du Roscoat S, Esnault Filet A, Garandet A. Characterization of contact properties in biocemented sand using 3D X-ray micro-tomography. Acta Geotech. 2019;14(3):597–613.

Dadda A, Geindreau C, Emeriault F, du Roscoat SR, Garandet A, Sapin L, et al. Characterization of microstructural and physical properties changes in biocemented sand using 3D X-ray microtomography. Acta Geotech. 2017;12(5):955–70.

Dawoud O. The Applicability of Microbially Induced Calcite Precipitation (MICP) for Soil Treatment. Cambridge: University of Cambridge, 2015. [Dissertation]

Dawoud O, Chen CY, Soga K. Microbial Induced Calcite Precipitation for Geotechnical and Environmental Applications. In: Geo-Shanghai 2014. Shanghai, China; 2014. p. 11–8.

DeJong JT, Fritzges MB, Nüsslein K. Microbially induced cementation to control sand response to undrained shear. J Geotech Geoenvironmental Eng. 2006;132(11):1381–92.

DeJong JT, Mortensen BM, Martinez BC, Nelson DC. Bio-mediated soil improvement. Ecol Eng. 2010;36(2):197–210.

DeJong JT, Soga K, Banwart SA, Whalley WR, Ginn TR, Nelson DC, et al. Soil engineering in vivo: Harnessing natural biogeochemical systems for sustainable, multi-functional engineering solutions. J R Soc Interface. 2011;8(54):1–15.

Dobereiner L. Engineering Geology of Weak Sanstones. London: Imperial College of Science and Technology, 1984. [Dissertation]

Elhakim AF. The use of point load test for Dubai weak calcareous sandstones. J Rock Mech Geotech Eng. 2015;7(4):452–7.

Feng K, Montoya BM. Influence of confinement and cementation level on the behavior of microbial-induced calcite precipitated Sands under monotonic drained loading. J Geotech Geoenvironmental Eng. 2015;142(1):04015057.

Fjar E, Holt RM, Raaen AM, Horsrud P. Petroleum Related Rock Mechanics. 2nd Edition. Vol. 53, Developments in Petroleum Science. Elsevier Science; 2008.

Freitas MH De, Dobereiner L. Geotechnical properties of weak sandstones. Géotechnique.

1986;36(1):79–94.

Gray. The packing of solid particles. London: Chapman and Hall; 1968.

Haimson B, Lee H. Borehole breakouts and compaction bands in two high-porosity sandstones. Int J Rock Mech Min Sci. 2004;41(2):287–301.

Harbottle MJ, Botusharova SP, Gardner DR. Self-healing soil: Biomimetic engineering of geotechnical structures to respond to damage. In: Proceedings of the 7th International Congress on Environmental Geotechnics. Melbourne, Australia; 2014. p. 1121–1128.

Heath LJ. Variations in Permeability and Porosity of Synthetic Oil Reservoir Rock—Methods of Control. Soc Pet Eng J. 1965;5(4):329–32.

Huang AB, Pan IW, Liao JJ, Wang CH, Hsieh SY. Pressuremeter tests in poorly cemented weak rocks. Am Rock Mech Assoc. 1999;247–52.

Ismail MA, Joer HA, Randolph MF, Meritt A. Cementation of porous materials using calcite. Géotechnique. 2002;52(5):313–24.

Ispas I, Eve R, Hickman RJ, Keck RG, Willson SM, Olson KE. SPE 159262 Laboratory Testing and Numerical Modelling of Fracture Propagation from Deviated Wells in Poorly Consolidated Formations. Spe [Internet]. 2012;1–16. Available from: https://www.onepetro.org/conference-paper/SPE-159262-MS

ISRM. Basic geotechnical description of rock masses. Int J Rock Mech Min Sci. 1981;(18):85–110.

Jiang N-J, Soga K. The applicability of microbially induced calcite precipitation (MICP) for internal erosion control in gravel–sand mixtures. Géotechnique [Internet]. 2017;67(1):42–55. Available from: http://www.icevirtuallibrary.com/doi/10.1680/jgeot.15.P.182

Jiang N-J, Soga K, Kuo M. Microbially Induced Carbonate Precipitation for Seepage-Induced

Internal Erosion Control in Sand–Clay Mixtures. J Geotech Geoenvironmental Eng [Internet]. 2017;143(3):04016100. Available from: http://ascelibrary.org/doi/10.1061/%28ASCE%29GT.1943-5606.0001559

Kanji MA. Engineering works affected by soft rocks. In: ISRM Conference on Rock Mechanics for Natural Resources and Infrastructure, SBMR 2014. Goiania, Brazil: 2014.

Konstantinou C. Hydraulic fracturing of artificially generated soft sandstones. Cambridge: University of Cambridge, 2020. [Dissertation]

Konstantinou C, Biscontin G. Soil enhancement via microbially induced calcite precipitation. In: Proceedings of the 10th International Symposium on Geotechnical Aspects of Underground Construction in Soft Ground. Cambridge: Taylor & Francis; 2020 (accepted paper).

Krishnan GR, Zhao XL, Zaman M, Roegiers JC. Fracture toughness of a soft sandstone. Int J Rock Mech Min Sci. 1998;35(6):695–710.

Krynine DP, Judd WR. Principles of Engineering Geology and Geotechnics. New York: McGraw-Hill, 1957.

Ku CS, Lee DH, Liao JJ, Wu JH. A case study of pile loading tests in poorly cemented rock. 42nd US Rock Mech Symp. 2008

Larsen EB. Geomechanical and Structural characteristics of of a paleoreservoir-caprock sucsession. Oslo: University of Oslo, 2015. [Dissertation]

Li M, Cheng X, Guo H. Heavy metal removal by biomineralization of urease producing bacteria isolated from soil. Int Biodeterior Biodegrad [Internet]. 2013;76:81–5. Available from: http://dx.doi.org/10.1016/j.ibiod.2012.06.016

Lin H, Suleiman MT, Brown DG, Kavazanjian E. Mechanical Behavior of Sands Treated by

Microbially Induced Carbonate Precipitation. J Geotech Geoenvironmental Eng. 2015;142(2):04015066.

Liu N, Skauge T, Landa-Marbán D, Hovland B, Thorbjørnsen B, Radu FA, et al. Microfluidic study of effects of flow velocity and nutrient concentration on biofilm accumulation and adhesive strength in the flowing and no-flowing microchannels. J Ind Microbiol Biotechnol. 2019;

Maccarini M. Laboratory Studies of a Weakly Bonded Artificial Soil. London: Imperial College of Science and Technology, 1987. [Dissertation]

Mahawish A, Bouazza A, Gates WP. Improvement of Coarse Sand Engineering Properties by Microbially Induced Calcite Precipitation. Geomicrobiol J [Internet]. 2018;35(10):887–97. Available from: https://doi.org/10.1080/01490451.2018.1488019

Martinez BC, DeJong JT, Ginn TR, Montoya BM, Barkouki TH, Hunt C, et al. Experimental Optimization of Microbial-Induced Carbonate Precipitation for Soil Improvement. J Geotech Geoenvironmental Eng. 2013;139(4):587–98.

Mitchell JK, Santamarina JC. Biological Considerations in Geotechnical Engineering. J Geotech Geoenvironmental Eng [Internet]. 2005;131(10):1222–33. Available from: http://ascelibrary.org/doi/10.1061/%28ASCE%291090-0241%282005%29131%3A10%281222%29

Mohlala K. Effects of Porosity on Strength of Sandstones (Hammanskraal and Waterberg). University of Pretoria, 2016. [Dissertation]

Montoya BM, DeJong JT. Stress-Strain Behavior of Sands Cemented by Microbially Induced Calcite Precipitation. J Geotech Geoenvironmental Eng. 2015;141(6):1–10.

Montoya BM, DeJong JT, Boulanger RW. Dynamic response of liquefiable sand improved by microbial-induced calcite precipitation. Géotechnique [Internet]. 2013;63(4):302–12.

Available from: http://www.icevirtuallibrary.com/content/article/10.1680/geot.SIP13.P.019

Mortensen BM, Haber MJ, Dejong JT, Caslake LF, Nelson DC. Effects of environmental factors on microbial induced calcium carbonate precipitation. J Appl Microbiol. 2011;111(2):338–49.

Mugwar AJ, Harbottle MJ. Toxicity effects on metal sequestration by microbially-induced carbonate precipitation. J Hazard Mater [Internet]. 2016;314:237–48. Available from: http://dx.doi.org/10.1016/j.jhazmat.2016.04.039

Mujah D, Shahin MA, Cheng L. State-of-the-Art Review of Biocementation by Microbially Induced Calcite Precipitation (MICP) for Soil Stabilization. Geomicrobiol J [Internet]. 2017;34(6):524–37. Available from: https://doi.org/10.1080/01490451.2016.1225866

Nakagawa S, Myer LR. Mechanical and acoustic properties of weakly cemented granular rocks. In: The 38th US Symposium on Rock Mechanics (USRMS). 2001. p. 1–8.

van Paassen L. Biogrout: Ground Improvement by Microbially Induced Carbonate Precipitation. Technology. Delft University of Technology; 2009. [Dissertation]

van Paassen LA, Ghose R, van der Linden TJM, van der Star WRL, van Loosdrecht MCM. Quantifying Biomediated Ground Improvement by Ureolysis: Large-Scale Biogrout Experiment. J Geotech Geoenvironmental Eng. 2010;136(12):1721–8.

Plumb RA. Influence of composition and texture on the failure properties of clastic rocks. In: Eurock SPE/ISRM Rock Mechanics in Petroleum Engineering. Delft, The Netherlands: Society of Petroleum Engineers; 1994. p. 13–9.

Pradhan S, Stroisz AM, Fjær E, Stenebraten J, Lund HK, Sønstebø EF, et al. Fracturing tests on reservoir rocks: Analysis of AE events and radial strain evolution. 48th US Rock Mech / Geomech Symp 2014. 2014;1:45–9.

Al Qabany A, Soga K. Effect of chemical treatment used in MICP on engineering properties of cemented soils. Geotechnique. 2013;63(4):331–9.

Al Qabany A, Soga K, Santamarina C. Factors Affecting Efficiency of Microbially Induced Calcite Precipitation. J Geotech Geoenvironmental Eng. 2012;138(8):992–1001.

Rabat, Cano M, Tomás R, Tamayo E, Alejano LR. Evaluation of Strength and Deformability of Soft Sedimentary Rocks in Dry and Saturated Conditions Through Needle Penetration and Point Load Tests: A Comparative Study. Rock Mech Rock Eng. 2020;1–28.

Rebata-Landa V. Microbial Activity in Sediments: Effects on Soil Behavior. Georgia Institute of Technology Atlanta, 2007. [Dissertation]

Rios S, Viana Da Fonseca A, Consoli NC, Floss M, Cristelo N. Influence of grain size and mineralogy on the porosity/cement ratio. Geotech Lett. 2013;3:130–6.

Saidi F, Bernabe Y, Reuschle T. The mechanical behaviour of synthetic, poorly consolidated granular rock under uniaxial compression. Tectonophysics. 2003;370:105–20.

Saidi F, Bernabé Y, Reuschlé T. Uniaxial compression of synthetic, poorly consolidated granular rock with a bimodal grain-size distribution. Rock Mech Rock Eng. 2005;38(2):129–44.

Sattler T, Paraskevopoulou C. Implications on Characterizing the Extremely Weak Sherwood Sandstone: Case of Slope Stability Analysis Using SRF at Two Oak Quarry in the UK. Geotech Geol Eng [Internet]. 2019;37(3):1897–918. Available from: https://doi.org/10.1007/s10706-018-0732-3

Shafii Rad N, Clough GW. The Influence of Cementation of the Static and Dynamic Behavior of Sands. Vol. 59. 1982.

Sharwood WJ. The specific gravity of mixtures (discussion). Econ Geol. 1912;7(6):588–90.

Sitar N, Clough GW, Bachus RG. Behavior of weakly cemented soil slopes under static and seismic loading conditions. 1980.

Suarez-Rivera R, Stenebråten J, Gadde PB, Sharma MM. An Experimental Investigation of Fracture Propagation During Water Injection. Int Symp Exhib Form Damage Control [Internet]. 2002; Available from: http://www.onepetro.org/doi/10.2118/73740-MS

Terzis D, Laloui L. Cell-free soil bio-cementation with strength, dilatancy and fabric characterization. Acta Geotech [Internet]. 2019;14(3):639–56. Available from: https://doi.org/10.1007/s11440-019-00764-3

Torres-Aravena ÁE, Duarte-Nass C, Azócar L, Mella-Herrera R, Rivas M, Jeison D. Can microbially induced calcite precipitation (MICP) through a ureolytic pathway be successfully applied for removing heavy metals from wastewaters? Crystals. 2018;8(11):1–13.

Umar M, Kassim KA, Ping Chiet KT. Biological process of soil improvement in civil engineering: A review. J Rock Mech Geotech Eng [Internet]. 2016;8(5):767–74. Available from: http://dx.doi.org/10.1016/j.jrmge.2016.02.004

Vogler D, Walsh SDC, Dombrovski E, Perras MA. A comparison of tensile failure in 3D-printed and natural sandstone. Eng Geol. 2017;226(June):221–35.

Wang Y, Soga K, Dejong JT, Kabla AJ. A microfluidic chip and its use in characterising the particle-scale behaviour of microbial-induced calcium carbonate precipitation (MICP). Géotechnique. 2019a;69(2):1086–94.

Wang Y, Soga K, Dejong JT, Kabla AJ. Micro-Scale Visualization of Microbial-Induced Calcium Carbonate Precipitation Processes. J Geotech Geoenvironmental Eng. 2019b;145(9):04019045.

Whiffin VS. Microbial CaCO3 Precipitation for the Production of Biocement. Perth, Western

Australia: Murdor University, 2004. [Dissertation]

Whiffin VS, van Paassen LA, Harkes MP. Microbial carbonate precipitation as a soil improvement technique. Geomicrobiol J. 2007;24(5):417–23.

Wygal RJ. Construction of Models that Simulate Oil Reservoirs. Soc Pet Eng J. 1963;3(04):281–6.

Zhao Q, Li L, Li C, Li M, Amini F, Zhang H. Factors Affecting Improvement of Engineering Properties of MICP-Treated Soil Catalyzed by Bacteria and Urease. J Mater Civ Eng [Internet]. 2014;26(2004):1–10. Available from: http://www.scopus.com/inward/record.url?eid=2-s2.0-84911865840&partnerID=tZOtx3y1